Nullifying ACF Grating Lobes in Stepped-Frequency Train of LFM Pulses

NADAV LEVANON, Fellow, IEEE
ELI MOZESON
Tel Aviv University

An effective way to increase the bandwidth of a coherent pulse-train is to add a frequency step Δf between consecutive pulses. A large Δf implies a large total bandwidth, hence improved range resolution. However, when the product of the frequency step times the pulse-duration t_p, is larger than one ($t_p\Delta f > 1$), the autocorrelation function (ACF) of the stepped-frequency pulse-train suffers from ambiguous peaks, known as "grating lobes." It is well known that replacing the fixed-frequency pulses with linear FM (LFM) pulses of bandwidth B can reduce those grating lobes. We present a simple analytic expression for the ambiguity function (AF) and ACF of such a signal and derive from it very simple relationships between Δf, B, and t_p that will place nulls exactly where the grating lobes are located, and thus remove them completely.

Manuscript received July 19, 2002; revised December 5, 2002; released for publication March 14, 2003.

IEEE Log No. T-AES/39/2/813113.

Refereeing of this contribution was handled by P. Lombardo.

Authors' address: Dept. of Electrical Engineering–Systems, Tel Aviv University, PO Box 39040, Tel Aviv 69978, Israel.

I. INTRODUCTION

Range resolution in radar is inversely related to the signal bandwidth. A coherent train of stepped-frequency pulses is an efficient method to achieve large overall bandwidth while maintaining narrow instantaneous bandwidth. One advantage of such an approach is that it allows utilizing the interval between pulses to adjust the center frequency of other narrow band components of the radar system, e.g., a phased array. One difficulty with this signal is the grating lobes that appear in the range response if $t_p\Delta f > 1$. Replacing the fix-frequency pulses with linear FM (LFM) pulses is known to lower those grating lobes. A stepped-frequency train of LFM pulses is sometimes called frequency-jumped burst (FJB). It is one of the waveforms used in the Target Resolution and Discrimination Experiment (TRADEX) radar, operating from the Kwajalein Atoll in the central Pacific Ocean [1].

The amplitude and frequency of a train of stepped-frequency LFM pulses is schematically depicted in Fig. 1. It is constructed from N pulses, each of duration t_p, with pulse repetition interval t_r. Each pulse is LFM with bandwidth B, and the center frequency step between pulses is Δf.

Methods to further lower range sidelobes and grating lobes in this type of signal were recently discussed [2–4]. In [2, 3] grating lobes are reduced by varying the pulsewidths, thus destroying the periodicity. The main theme in [4] is to use variable frequency steps according to a nonlinear law. This mitigates grating lobes and reshapes the spectrum resulting in a reduction of range sidelobes as well.

In the work presented here, t_p, Δf, and B remain constant throughout the pulse train. However the relationship between these three parameters is set in such a way that the grating lobes disappear. Toward that purpose we need to develop the autocorrelation function (ACF) of the signal. It turns out that it is simpler to develop the ambiguity function (AF) first. Note that even with fixed parameters, when $B > \Delta f > 0$, the overall spectrum is not uniform anymore, but shaped in a way that emphasizes the center of the band.

II. AMBIGUITY FUNCTION OF STEPPED-FREQUENCY LFM PULSES

We begin with the AF of a single LFM pulse whose complex envelope $u_1(t)$ has unit energy

$$u_1(t) = \frac{1}{\sqrt{t_p}}\text{rect}\left(\frac{t}{t_p}\right)\exp(j\pi kt^2) \tag{1}$$

where k is the frequency slope, related to the bandwidth B_1 (>0) of the single pulse according to

$$k = \pm\frac{B_1}{t_p} \tag{2}$$

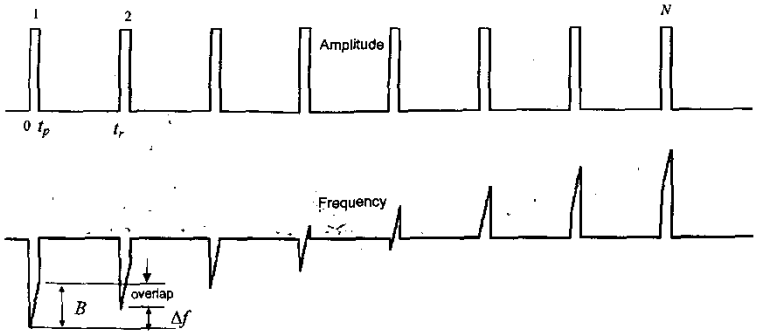

Fig. 1. Stepped-frequency LFM pulses.

where a "+" sign stands for a positive frequency slope and a "−" sign stands for a negative frequency slope. Henceforth we assume a positive frequency slope ($k > 0$), but the results apply to a negative slope as well. Note that k and B_1 are not the ultimate values of the single pulse slope and bandwidth. For the sake of brevity we also use the following notation:

$$\operatorname{sinc}(x) = \frac{\sin(\pi x)}{\pi x}.$$

The AF of such a single LFM pulse is well known (see e.g., [5])

$$|\chi_1(\tau,\nu)| = \left|\left(1-\frac{|\tau|}{t_p}\right)\operatorname{sinc}\left[t_p(\nu+k\tau)\left(1-\frac{|\tau|}{t_p}\right)\right]\right|, \qquad |\tau| \le t_p. \tag{3}$$

Next we create a uniform pulse train of N such LFM pulses separated by $t_r > 2t_p$

$$u_N(t) = \frac{1}{\sqrt{N}}\sum_{n=0}^{N-1} u_1(t-nt_r). \tag{4}$$

Unit energy is maintained due to the division by $\sqrt{N}$. For delay τ shorter than the pulse duration t_p, the AF of the coherent pulse train is related to the AF of a single pulse according to

$$|\chi_N(\tau,\nu)| = |\chi_1(\tau,\nu)|\left|\frac{\sin(N\pi\nu t_r)}{N\sin(\pi\nu t_r)}\right|, \qquad |\tau| \le t_p. \tag{5}$$

We now add LFM to the entire train of pulses, using an additional (but different) slope k_s

$$u_S(t) = u_N(t)\exp(j\pi k_s t^2) = \frac{1}{\sqrt{N}}\exp(j\pi k_s t^2)\sum_{n=0}^{N-1} u_1(t-nt_r) \tag{6}$$

where

$$k_s = \pm\frac{\Delta f}{t_r}, \qquad \Delta f > 0 \tag{7}$$

where a "+" sign stands for a positive frequency step and a "−" sign stands for a negative frequency step. Henceforth we will assume a positive frequency step ($k_s > 0$), but the results apply to a negative step as well. Adding LFM to a signal modifies its AF according to a simple rule [5]

$$|\chi_S(\tau,\nu)| = |\chi_N(\tau,\nu+k_s\tau)|. \tag{8}$$

Applying (8) to (5) we get

$$|\chi_S(\tau,\nu)| = |\chi_1(\tau,\nu+k_s\tau)|\left|\frac{\sin[N\pi(\nu+k_s\tau)t_r]}{N\sin[\pi(\nu+k_s\tau)t_r]}\right|, \qquad |\tau| \le t_p. \tag{9}$$

Using (3) in (9) we get the AF of the combined signal

$$|\chi_{NS}(\tau,\nu)| = \left|\left(1-\frac{|\tau|}{t_p}\right)\operatorname{sinc}\left[t_p[\nu+(k+k_s)\tau]\left(1-\frac{|\tau|}{t_p}\right)\right]\right| \times \left|\frac{\sin[N\pi(\nu+k_s\tau)t_r]}{N\sin[\pi(\nu+k_s\tau)t_r]}\right|, \qquad |\tau| \le t_p. \tag{10}$$

Note that the LFM slope k_s, introduced to create the frequency step, adds to the original slope k of the single LFM pulse. Hence the ultimate bandwidth of each pulse in the train is

$$B = |k + k_s|t_p. \tag{11}$$

Using (7) and (11) in (10) the AF expression is simplified to

$$|\chi_{NS}(\tau,\nu)| = \left|\left(1-\frac{|\tau|}{t_p}\right)\operatorname{sinc}\left[t_p\left(\nu+B\frac{\tau}{t_p}\right)\left(1-\frac{|\tau|}{t_p}\right)\right]\right| \times \left|\frac{\sin\left[N\pi\left(\nu+\Delta f\frac{\tau}{t_r}\right)t_r\right]}{N\sin\left[\pi\left(\nu+\Delta f\frac{\tau}{t_r}\right)t_r\right]}\right|, \qquad |\tau| \le t_p. \tag{12}$$

III. NULLIFYING GRATING LOBES

We now nullify the grating lobes at the zero Doppler cut of the AF, which is also the magnitude of the ACF $R(\tau)$. $|R(\tau)|$ is obtained by setting $\nu = 0$ in (12) yielding

$$|R(\tau)| = \left|\left(1-\frac{|\tau|}{t_p}\right)\operatorname{sinc}\left[B\tau\left(1-\frac{|\tau|}{t_p}\right)\right]\right|\left|\frac{\sin(N\pi\tau\Delta f)}{N\sin(\pi\tau\Delta f)}\right|, \qquad |\tau| \le t_p. \tag{13}$$

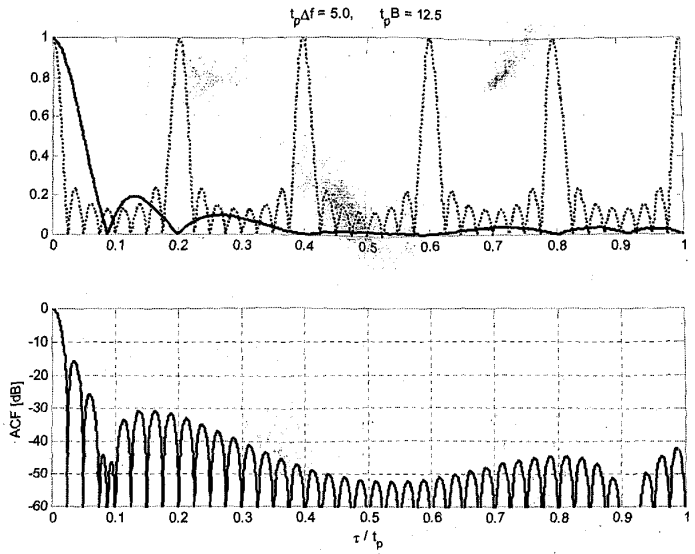

Fig. 2. Stepped-frequency train of LFM pulses with grating lobe cancellation. Top: $|R_1(\tau)|$ (solid) and $|R_2(\tau)|$ (dash). Bottom: partial ACF (in dB). $N = 8$, $t_p\Delta f = 5$, $t_pB = 12.5$

Equation (13) is a product of two terms. The first is due to a single LFM pulse with increased slope

$$|R_1(\tau)| = \left|\left(1-\frac{|\tau|}{t_p}\right)\operatorname{sinc}\left[B\tau\left(1-\frac{|\tau|}{t_p}\right)\right]\right|, \quad |\tau| \le t_p. \tag{14}$$

The second term describes the grating lobes

$$|R_2(\tau)| = \left|\frac{\sin(N\pi\tau\Delta f)}{N\sin(\pi\tau\Delta f)}\right|, \qquad |\tau| \le t_p. \tag{15}$$

Clearly $|R_2(\tau)|$ exhibits peaks (mainlobe and grating lobes) at

$$\tau_{\text{lobes}} = \frac{g}{\Delta f}, \qquad g = 0, \pm 1, \pm 2, \ldots, \lfloor t_p\Delta f \rfloor, \quad |\tau| < t_p \tag{16}$$

where $\lfloor x \rfloor$ implies the largest integer not exceeding x.

Nullifying the grating lobes of $|R_2(\tau)|$ is based on requiring that the nulls of $|R_1(\tau)|$ coincide with them. Finding such cases is based on requiring coincidence in two of the grating lobes. In some cases this requirement nullifies all the grating lobes.

The general procedure is discussed in Section VI, while here we present a simple example. Requiring that $|R_1(\tau)|$ will exhibit it's 2nd and 3rd nulls exactly at the first two gratings lobes, namely at $\tau = 1/\Delta f$ and $\tau = 2/\Delta f$, respectively, yields the following two relationships:

$$t_p\Delta f = 5 \tag{17}$$

and

$$t_pB = 12.5. \tag{18}$$

The relationship in (17) implies that there must be exactly five grating lobes within the pulse duration. It turns out, however, that in this case, as in many others, not only the first two grating lobes are nullified when conditions (17) and (18) are met, but all five grating lobes are nullified. This property is demonstrated in Fig. 2 (top) where $|R_1(\tau)|$ and $|R_2(\tau)|$ are plotted on top of each other (for $0 \le \tau \le t_p$). The resulting magnitude of the ACF on a logarithmic scale is plotted in Fig. 2 (bottom). No grating lobes can be seen. For comparison the ACF obtained with fixed-frequency pulses is presented in Fig. 3, where the grating lobes are prominent. Note that Figs. 2 and 3 were obtained using $N = 8$ pulses, which explains the 6 smaller lobes easily observed between every two grating lobes in Figs. 2 and 3. Other than that dependence on N, the figures are universal in the sense that they are functions only of t_pB and $t_p\Delta f$.

IV. AMBIGUITY FUNCTION PLOTS

It is interesting to look at the AF of stepped-frequency pulse-trains, with LFM (whose parameters are set according to (17) and (18)) and without LFM. The two plots are presented in Figs. 4 and 5, respectively. Again the AFs were plotted for a signal with $N = 8$ pulses. However here we need to specify the duty cycle which was $t_p/t_r = 1/9$. In both figures $t_p\Delta f = 5$. In Fig. 4 $t_pB = 12.5$. Note that Nt_r, which normalizes the Doppler axis, is the entire duration of the signal.

Fig. 4 shows that the nullifying is effective for extended Doppler. The grating lobes build-up with Doppler is relatively slow. This behavior is typical of all the cases discussed here. Comparing Figs. 4 and 5

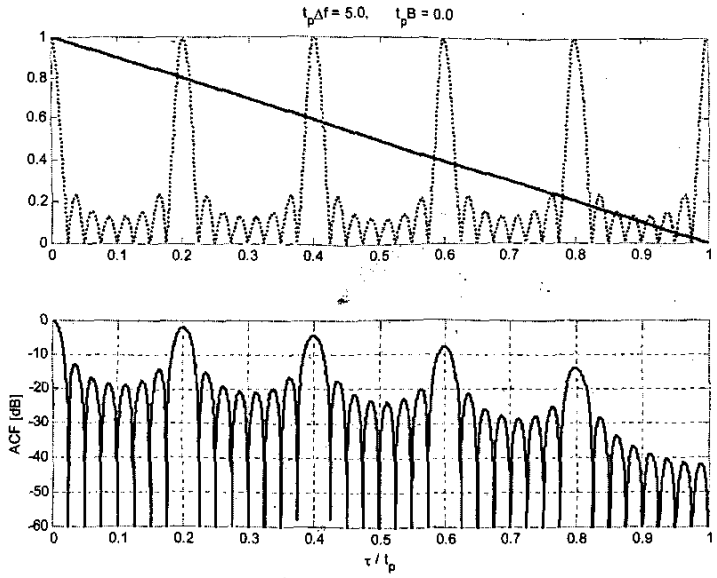

Fig. 3. Stepped-frequency train of fixed-frequency pulses. Top: $|R_1(\tau)|$ (solid) and $|R_2(\tau)|$ (dash). Bottom: partial ACF (in dB). $N = 8$, $t_p\Delta f = 5$, $t_pB = 0$.

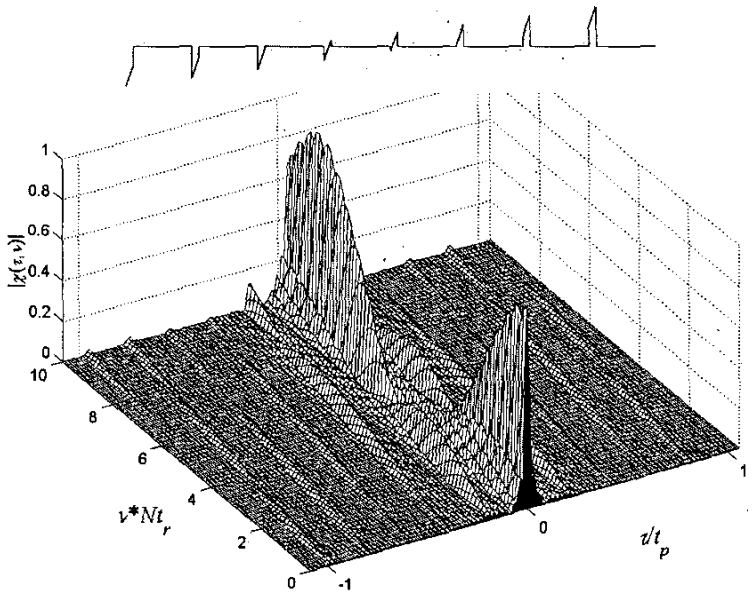

Fig. 4. Ambiguity function of stepped-frequency train of LFM pulses with grating lobe cancellation. Delay axis limited to $|\tau| \le t_p$. $N = 8$, $t_p\Delta f = 5$, $t_pB = 12.5$, $t_r/t_p = 9$.

we also note that the height of the main diagonal ridge (around zero delay) of the AF in Fig. 5 decays very slowly with Doppler; while in Fig. 4 the ridge height decays faster.

Comparing Figs. 4 and 5, the volume underneath the AF, removed from the strip $|\tau| \le t_p$, must show up elsewhere. It will be found in the recurrent lobes (around multiples of t_r). As Fig. 1 shows, having $B > \Delta f$ creates some frequency overlap between pulses despite the frequency steps. Such an overlap does not exist with fixed-frequency pulses. The overlap is responsible for the relatively strong AF peaks at multiples of t_r. Figs. 6 and 7 extend the delay axis of Figs. 4 and 5, to include the first recurrent lobes, and confirm the conclusion stated here. The AF volume distribution in the recurrent lobes depends on the order of pulses. If the pulse order is permuted, the volume in the recurrent lobes will be redistributed. Note that rearranging the order of pulses does not alter the ACF for $|\tau| \le t_p$, hence does not affect the nullifying process, which is confined to this delay span.

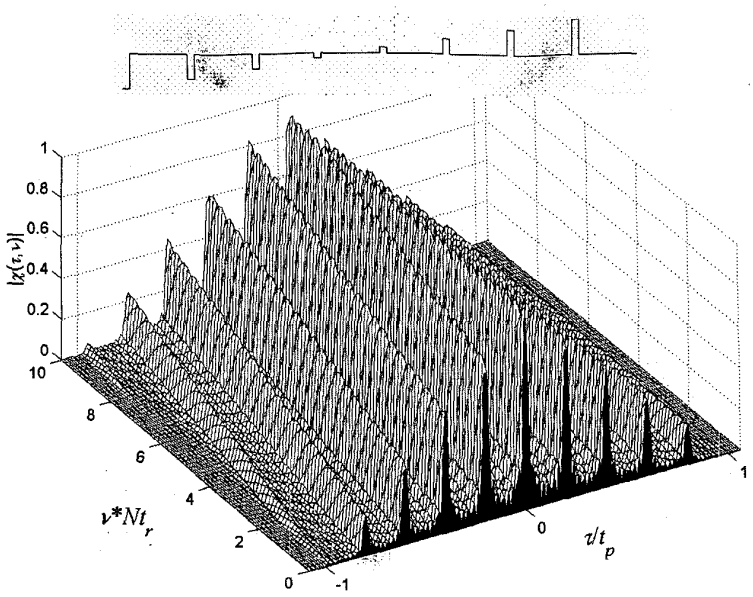

Fig. 5. Ambiguity function of stepped-frequency train of fixed-frequency pulses. Delay axis limited to $|\tau| \leq t_p$. $N = 8$, $t_p\Delta f = 5$, $t_pB = 0$, $t_r/t_p = 9$.

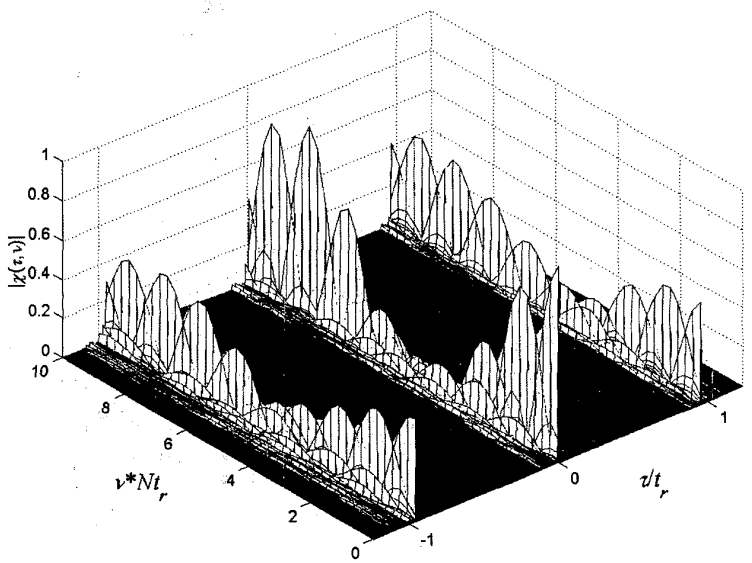

Fig. 6. Ambiguity function of stepped-frequency train of LFM pulses with grating lobe cancellation. Delay axis extended to include the nearest recurrent lobes. $N = 8$, $t_p\Delta f = 5$, $t_pB = 12.5$, $t_r/t_p = 9$.

For comparison with Figs. 4 and 5, Fig. 8 presents the well-known AF of a train of identical LFM pulses (no frequency steps). Each pulse has the same total frequency deviation as the combined frequency deviation $B + (N-1)\Delta f$ of the entire train of stepped-frequency LFM pulses. Fig. 8 displays the well known Doppler resolution of a coherent train of 8 identical pulses. Such Doppler resolution is completely lost in stepped-frequency pulse train (Fig. 5), and partially lost in our stepped-frequency train of LFM pulses.

V. SPECIAL CASES WHEN $t_p\Delta f \leq 3$

Before presenting a general search method for parameters which results in nullifying the grating lobes, we discuss the special case in which $t_p\Delta f \leq 3$, namely when there are no more than three grating lobes (positive delay). These cases are affected by the symmetry about $\tau = t_p/2$ of the sine argument in (14), $\pi B\tau(1 - |\tau|/t_p)$.

Inserting the location of the first grating lobe $\tau_1 = 1/\Delta f$ in the expression of the sine argument and equating it to π will place the first null on the first

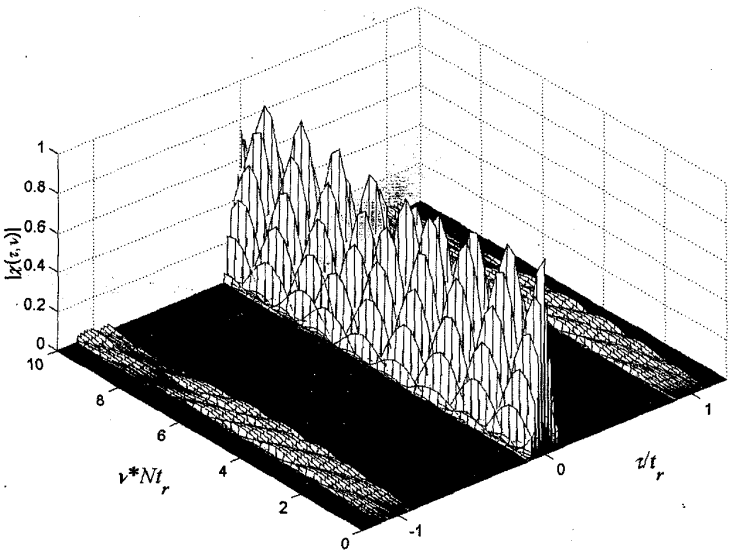

Fig. 7. Ambiguity function of stepped-frequency train of fixed-frequency pulses. Delay axis extended to include the nearest recurrent lobes. $N = 8$, $t_p\Delta f = 5$, $t_pB = 0$, $t_r/t_p = 9$.

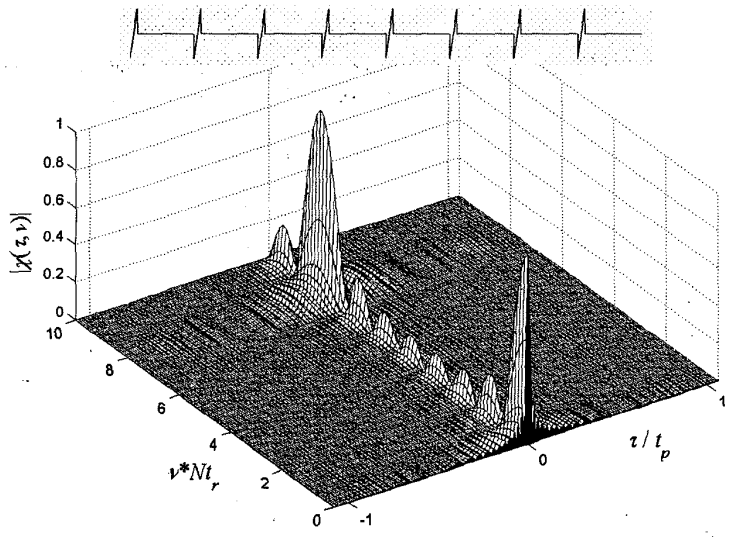

Fig. 8. Ambiguity function of a train of identical LFM pulses. Delay axis limited to $|\tau| \le t_p$. $N = 8$, $t_p\Delta f = 0$, $t_pB = 47.5$, $t_r/t_p = 9$.

grating lobe. The resulting relationship is

$$t_pB = \frac{(t_p\Delta f)^2}{t_p\Delta f - 1}. \tag{19}$$

When $1 < t_p\Delta f \le 2$ the first grating lobe is located in the second half of the pulse duration $t_p/2 < \tau_1 < t_p$, placing a null on it will also place a symmetrical null in the first half, where there is no grating lobe. An example is shown in Fig. 9. Clearly in this case it is impossible to match the first grating lobe with the first null, but it is possible to match a null for any location of the single grating lobe, hence $t_p\Delta f$ can take any value within the limits $1 < t_p\Delta f \le 2$. (For the specific value of $t_p\Delta f = 2$ and $t_pB = 4$, the first and second null coincide at $t_p/2$, hence the first grating lobe matches both the first and second null, and the second grating lobe, at $\tau_2 = t_p$, matches the third null.)

When $2 < t_p\Delta f \le 3$ the first grating lobe is located in the first half of the pulse duration $0 < \tau_1 < t_p/2$, placing a null on it using (19) will place also a symmetrical null in the second half. For that second null to match the second grating lobe, located at $\tau_2 = 2/\Delta f$, it is necessary that the following will also hold

$$t_pB = \frac{(t_p\Delta f)^2}{2(t_p\Delta f - 2)}. \tag{20}$$

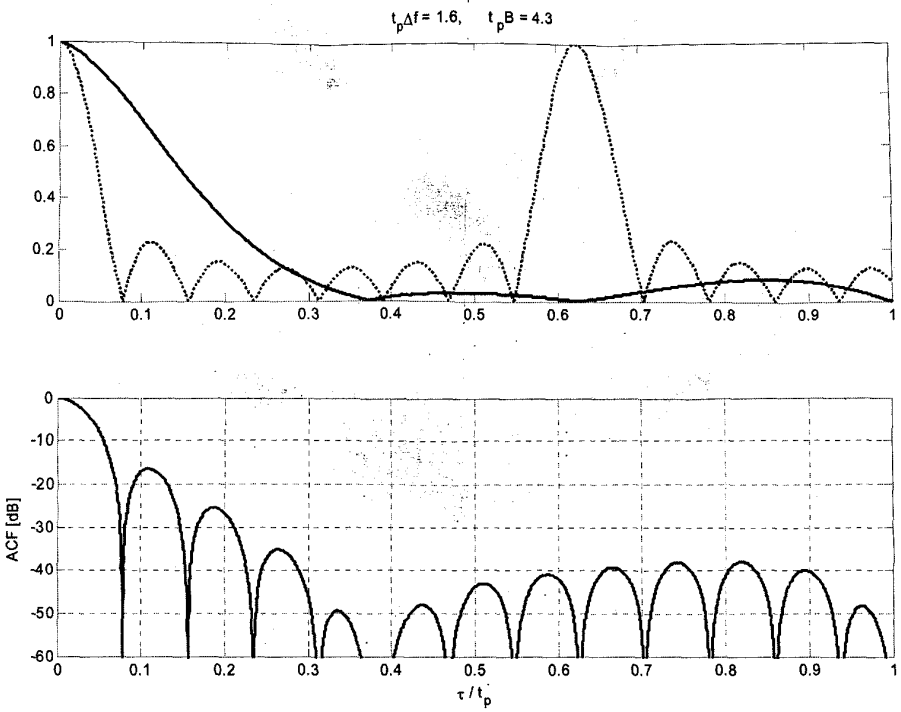

Fig. 9. Stepped-frequency train of LFM pulses with grating lobe cancellation. Top: $|R_1(\tau)|$ (solid) and $|R_2(\tau)|$ (dash). Bottom: partial ACF (in dB). $N = 8$, $t_p\Delta f = 1.6$, $t_pB = 4.27$.

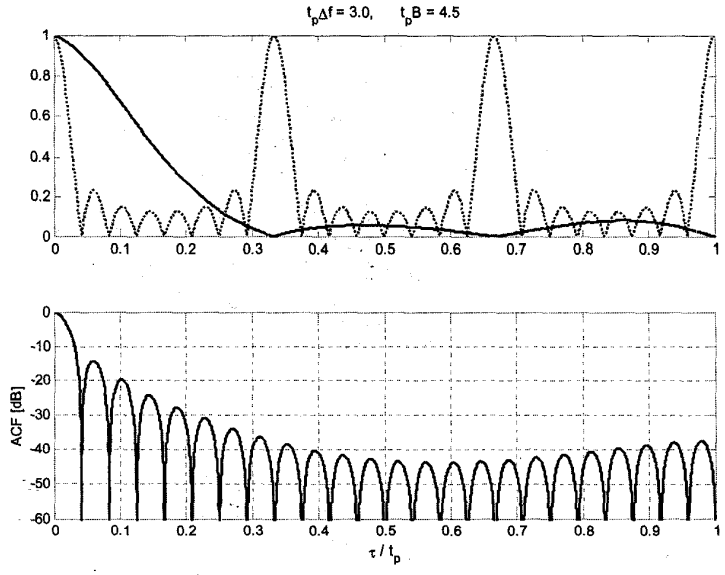

Fig. 10. Stepped-frequency train of LFM pulses with grating lobe cancellation. Top: $|R_1(\tau)|$ (solid) and $|R_2(\tau)|$ (dash). Bottom: partial ACF (in dB). $N = 8$, $t_p\Delta f = 3$, $t_pB = 4.5$.

Both (19) and (20) will hold true only when $t_p\Delta f = 3$ and $t_pB = 4.5$. This case is shown in Fig. 10. It is the only case in which the first two grating lobes match the first two nulls. When $t_p\Delta f > 3$ there are three or more grating lobes, and matching nulls to the first two is more regular. A search procedure is described next.

VI. GENERAL SEARCH PROCEDURE

The search procedure tries to find coincidences between two grating lobes of $|R_2(\tau)|$ and two nulls of $|R_1(\tau)|$ when $t_p\Delta f > 3$. In some of the cases the coincidence will hold for all the grating lobes of $|R_2(\tau)|$.

A step in the search requires that $|R_1(\tau)|$ exhibits it's mth and nth ($n \geq m$) nulls exactly at the qth and rth ($r > q$) gratings lobes, namely at $\tau = q/\Delta f$ and $\tau = r/\Delta f$, respectively. The entire search goes through all the possible choices of m, n, q, and r, that meet the constraints above. Using a specific choice of m, n, q, and r in (14) and (15) yields the following two relationships:

$$\pi B \frac{q}{\Delta f}\left(1 - \frac{q}{t_p \Delta f}\right) = m\pi \tag{21}$$

and

$$\pi B \frac{r}{\Delta f}\left(1 - \frac{r}{t_p \Delta f}\right) = n\pi. \tag{22}$$

Thus

$$\frac{r}{n}\left(1 - \frac{r}{t_p \Delta f}\right) = \frac{q}{m}\left(1 - \frac{q}{t_p \Delta f}\right). \tag{23}$$

Of special importance is the requirement to nullify the first two grating lobes, namely $q = 1$ and $r = 2$. Solving $t_p \Delta f$ yields

$$t_p \Delta f = \frac{mr^2 - nq^2}{mr - nq} \underset{q=1,r=2}{=} \frac{4m - n}{2m - n}. \tag{24}$$

Recall that n, m, q, and r should be all positive and that $m \leq n$ and $q < r$. Note that $\lfloor t_p \Delta f \rfloor$ is the number of grating lobes. To be a valid solution it must be positive and greater than r.

If a valid $t_p \Delta f$ was found for a specific selection of m, n, q, and r, using it in (22) leads to the pulse time-bandwidth product as

$$t_p B = \frac{n}{r(t_p \Delta f - r)}(t_p \Delta f)^2 = \frac{(mr^2 - nq^2)^2}{qr(r-q)(mr - nq)} \underset{q=1,r=2}{=} \frac{(4m-n)^2}{2(2m-n)}. \tag{25}$$

The ratio $B/\Delta f$, which we call overlap ratio (see Fig. 1) is

$$\frac{B}{\Delta f} = \frac{nt_p \Delta f}{r(t_p \Delta f - r)} = \frac{(mr^2 - nq^2)}{qr(r-q)} \underset{q=1,r=2}{=} \frac{4m-n}{2}. \tag{26}$$

The number of pulses N should be much greater than the overlap ratio in order to get a meaningful increase in bandwidth.

Once m, n, q, and r are selected (resulting with a given pulse time-bandwidth product and an overlap ratio) the ACF can be written as a function of $t_p B$ and $t_p \Delta f$:

$$\left|R\left(\frac{\tau}{t_p}\right)\right| = \left|\left(1 - \left|\frac{\tau}{t_p}\right|\right) \operatorname{sinc}\left[t_p B \frac{\tau}{t_p}\left(1 - \left|\frac{\tau}{t_p}\right|\right)\right]\right| \times \left|\frac{\sin\left(N\pi t_p \Delta f \frac{\tau}{t_p}\right)}{N \sin\left(\pi t_p \Delta f \frac{\tau}{t_p}\right)}\right|, \quad \left|\frac{\tau}{t_p}\right| \leq 1 \tag{27}$$

TABLE I
Examples of Valid Cases

m	n	q	r	$t_p \Delta f$	Bt_p	$B/\Delta f$
*	*	1	2	2	4	2
1	1	1	2	3	4.5	1.5
2	2	1	2	3	9	3
2	3	1	2	5	12.5	2.5
3	3	1	2	3	13.5	4.5
3	4	1	2	4	16	4
4	4	1	2	3	18	6
4	5	1	2	3.667	20.1667	5.5
5	6	1	2	3.5	24.5	7
4	7	1	2	9	40.5	4.5

where the dimensionless parameters $t_p B$ and $t_p \Delta f$ are functions of only m, n, q, and r. As pointed out before, the nulls of $|R_1(\tau)|$ are symmetrical around $\tau = t_p/2$. Note also that the number of nulls is the smallest integer no less than $t_p B/2$ (i.e., $\lceil t_p B/2 \rceil$). The number of peaks in $|R_2(\tau)|$ (grating lobes) is $\lfloor t_p \Delta f \rfloor$ (plus the mainlobe) and the peaks positions are symmetric around $\tau = t_p/2$ when $t_p \Delta f$ is an integer.

Samples from a numerical search for possible candidates for m, n, q, and r produced the parameters listed in Table I. (Only a few are listed. Many more exist). Table I includes cases in which nullifying two grating lobes resulted in nullifying all the grating lobes.

Table I contains only a small fraction of the integer values of m and n over which the search was performed. We scanned integer values of m and n such that $t_p B$ is as high as 2000 (m and n are from 1 to 1500) and found that for each value of $t_p B$ a solution is feasible only for relatively small values of $t_p \Delta f$. For example, for $t_p B = 1600$ we did not find $t_p \Delta f > 60$ that still nullifies the first and second grating lobe. This result implies that when $t_p B$ is large a valid frequency step Δf must be small, and the number of pulses N should be very large in order to get a noticeable increase in bandwidth.

In addition to the fact that the grating lobes were nullified, there is interest in the mainlobe width and the height of the near sidelobes. Both are affected also by the number of pulses N. Regarding the mainlobe width, the location of the first overall null is determined by which of the two expressions: $|R_1(\tau)|$ or $|R_2(\tau)|$, exhibits an earlier first null (see (14) and (15)). When $t_p B \gg 1$ the location of the first null of $|R_1(\tau)|$ is approximately the inverse of $t_p B$. This allows a simple expression for the location of the first overall null,

$$\frac{\tau_{\text{1st null}}}{t_p} = \min\left(\frac{1}{t_p B}, \frac{1}{Nt_p \Delta f}\right). \tag{28}$$

The height of the near sidelobes cannot be described by a simple expression. However, when

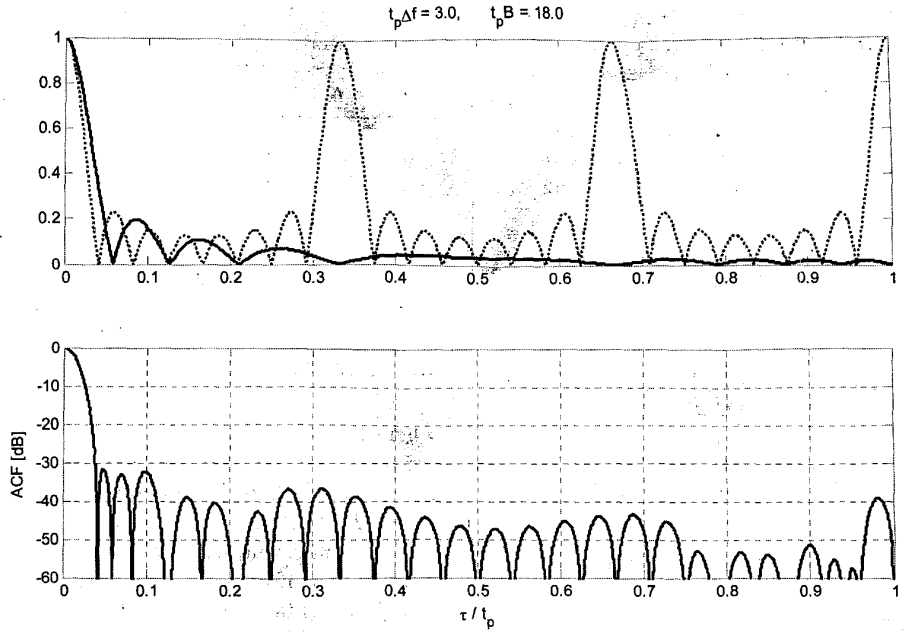

Fig. 11. Stepped-frequency train of LFM pulses with grating lobe cancellation. Top: $|R_1(\tau)|$ (solid) and $|R_2(\tau)|$ (dash). Bottom: partial ACF (in dB). $N = 8$, $t_p\Delta f = 3$, $t_pB = 18$.

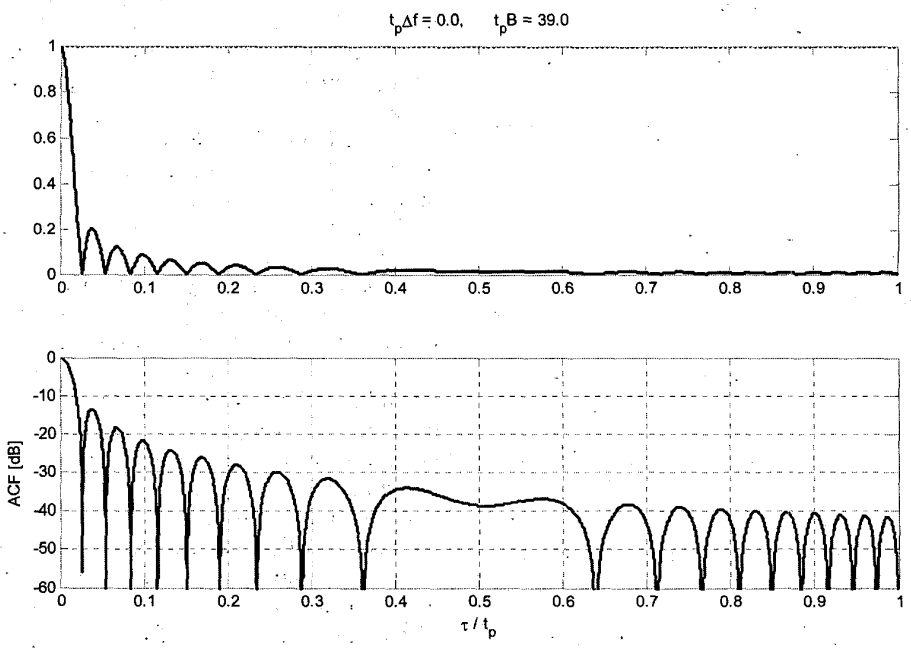

Fig. 12. ACF of train of identical LFM pulses with same total frequency deviation as signal in Fig. 11. Top: linear scale. Bottom: log scale (in dB). $N = 8$, $t_p\Delta f = 0$, $t_pB = 39$.

$t_pB \approx 2/3Nt_p\Delta f$ the first null of $|R_1(\tau)|$ will approximately coincide with the peak of the first (and highest) sidelobe of $|R_2(\tau)|$, splitting it into two lower sidelobes. An example is given in Fig. 11. Thus, in addition to nullifying the first grating lobes, we have used the additional parameter N to place a null on the first sidelobe peak.

In Fig. 11 we used the case: $m = 4$, $n = 4$, $q = 1$, $r = 2$, $t_p\Delta f = 3$, $t_pB = 18$. This results in $B/\Delta f = 6 \gg 1$, and a relatively large m. As $B/\Delta f$ and hence m are increased the mainlobe of the ACF will be determined more by $|R_1(\tau)|$ than by $|R_2(\tau)|$. In the limit, when $\Delta f = 0$, the signal reduces to a train of identical LFM pulses.

It is interesting to compare the ACF given in Fig. 11, with the ACF of a train of identical LFM pulses (no frequency steps), in which the entire bandwidth, $B + (N-1)\Delta f$, is put in each pulse. The ACF of such a signal is given in Fig. 12. Comparing the two figures we note that stepped LFM yields lower sidelobes and wider mainlobe. This is typical to the outcome of a weighted LFM and nonlinear FM. Both are designed to give more weight to the center frequencies. Indeed, as pointed out in the introduction, when $B > \Delta f > 0$ the spectrum emphasizes the center frequencies.

VII. CONCLUSIONS

Good range resolution requires wide bandwidth, which can be obtained relatively simply by using a stepped-frequency train of pulses. An associated difficulty, however, are "grating lobes" at delay intervals of $1/\Delta f$. Replacing the fixed-frequency individual pulses with LFM pulses can mitigate the grating lobes problem. We showed that imposing two specific relationships on the two signal parameters ($t_p B$ and $t_p \Delta f$) results in complete nullifying of the grating lobes. We presented a search procedure for these two relationships, and provided several examples. Our search revealed that for very large $t_p B$ a valid normalized frequency step $t_p \Delta f$ must be small; hence the number of pulses N should be very high in order to get a noticeable increase in bandwidth.

REFERENCES

[1] Ingwersen, P. E., Camp, W. W., and Fenn, A. J. (2002)
Radar technology for ballistic missile defense.
Lincoln Laboratory Journal, **13**, 1 (2002), 109–147.

[2] Maron, D. E. (1987)
Non-periodic frequency-jumped burst waveforms.
In *Proceedings of the IEE International Radar Conference*, London, Oct. 1987, 484–488.

[3] Maron, D. E. (1990)
Frequency-jumped burst waveforms with stretch processing.
In *Proceedings of the IEEE International Radar Conference*, Arlington, VA, May 1990, 274–279.

[4] Rabideau, D. J. (2002)
Nonlinear synthetic wideband waveforms.
In *Proceedings of the IEEE Radar Conference*, Los Angeles, May 2002, 212–219.

[5] Levanon, N. (1988)
Radar Principles.
New York: Wiley, 1988.

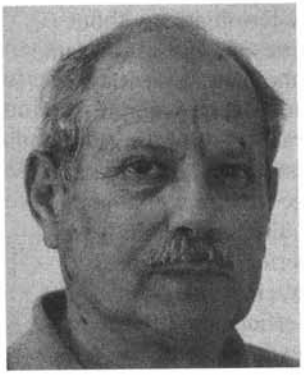

Nadav Levanon (S'67—M'70—SM'83—F'98) received a B.Sc. and M.Sc. degrees from the Technion–Israel Institute of Technology, in 1961 and 1965, and a Ph.D. from the University of Wisconsin–Madison, in 1969, all in electrical engineering.

He has been a faculty member at Tel Aviv University since 1970, where he is a professor in the Department of Electrical Engineering–Systems, and head of the Weinstein Research Institute for Signal Processing. He was chairman of the EE-Systems Department between 1983–1985. He spent sabbatical years at the University of Wisconsin, The Johns Hopkins University–Applied Physics Lab., and Qualcomm Inc., San Diego, CA.

Dr. Levanon is a member of the IEE, ION, and AGU. He is the author of the book *Radar Principles* (Wiley, 1988).

Eli Mozeson was born on May 26, 1970. He received his B.Sc. and M.Sc. degrees in electrical engineering from Tel-Aviv University, Israel, in 1992 and 1999, respectively. Since 1992 he serves in the Israeli Air Force as an electronic engineer. Currently, he is a Ph.D. student in the Department of Electrical Engineering–Systems, Tel-Aviv University. His area of interest is application of multicarrier phase-coded signals to radar systems.